

ExoMol molecular line lists X: The spectrum of sodium hydride

Tom Rivlin¹, Lorenzo Lodi¹, Sergei N. Yurchenko¹, Jonathan Tennyson¹,
Robert J. Le Roy²

¹*Department of Physics and Astronomy, University College London, London WC1E 6BT, UK;*

²*Department of Chemistry, University of Waterloo, Waterloo, Ontario N2L 3G1, Canada*

Accepted XXXX. Received XXXX; in original form XXXX

ABSTRACT

Accurate and complete rotational, rotational-vibrational and rotational-vibrational-electronic line lists are calculated for sodium hydride: both the NaH and NaD isotopologues are considered. These line lists cover all ro-vibrational states of the ground ($X\ ^1\Sigma^+$) and first excited ($A\ ^1\Sigma^+$) electronic states. The calculations use available spectroscopically-determined potential energy curves and new high-quality, *ab initio* dipole moment curves. Partition functions for both isotopologues are calculated and the effect of quasibound states is considered. The resulting line lists are suitable for temperatures up to about 7000 K and are designed for studies of exoplanet atmospheres, brown dwarfs and cool stars. In particular, the NaH $A - X$ band is found to show a broad absorption feature at about 385 nm which should provide a signature for the molecule. All partition functions, lines and transitions are available as Supplementary Information to this article and at www.exomol.com.

molecular data; opacity; astronomical data bases: miscellaneous; planets and satellites: atmospheres; stars: low-mass

1 INTRODUCTION

Although long discussed (Kirby & Dalgarno 1978), the existence of sodium hydride, NaH, is yet to be confirmed in any astronomical bodies. Notably few metal hydrides have been detected in the interstellar medium and searches for NaH in both dense clouds (Plambeck & Erickson 1982) and diffuse clouds (Snow & Smith 1977; Czarny et al. 1987) have so far only yielded upper limits. Similarly an attempt to detect the long-wavelength signature for NaH in the atmosphere of Jupiter and Saturn (Weisstein & Serabyn 1996) also proved negative.

While spectroscopic data for long-wavelength studies of NaH has been the subject of the laboratory studies (Leopold et al. 1987; Okabayashi & Tanimoto 2000), and are compiled in the CDMS database (Müller et al. 2005), the situation is less clear at infrared and visible wavelengths. A recent work on M-dwarf models by Rajpurohit et al. (2013) identified NaH as one of only three molecules for which the necessary spectroscopic data is missing. This is despite the fact that the $A - X$ band of NaH should give an observable feature at visible wavelengths. It is this situation we address here. We note that the next lowest-lying singlet electronic excited states of NaH are the $C\ ^1\Sigma^+$ (Walji et al. 2015) and the shallow $B\ ^1\Pi$ state (Yang et al. 2004) whose yet to be observed spectra lie in the ultraviolet, probably at around 3000 Å.

The large dipole moments of NaH, as well as supposedly making it more amenable to astronomical detection, has also excited the interest of scientists working on ultra-cold molecules (Juarros et al. 2006; Aymar et al. 2009; Su et al. 2010). In particular, it has been suggested that these dipoles should enhance the prospects of molecule formation by radiative association at very low temperatures (Juarros et al. 2006).

The ExoMol project aims to provide line lists of spectroscopic transitions for key molecular species which are likely to be important in the atmospheres of extrasolar planets and cool stars; its aims, scope and methodology have been summarised by Tennyson & Yurchenko (2012). In this paper, ro-vibrational and rovibronic transition lists are computed for the only two stable isotopes of sodium hydride, ²³NaH and ²³NaD. These line lists consider transitions within and between the two lowest electronic states of NaH, $X\ ^1\Sigma^+$ and $A\ ^1\Sigma^+$. The resulting line lists are comprehensive and should be valid up to the 7000 K temperature range.

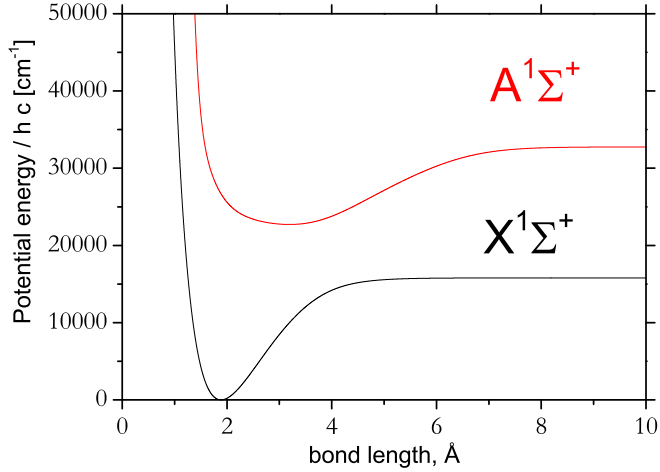


Figure 1. Empirical NaH $X^1\Sigma_g^+$ and $A^1\Sigma_g^+$ state potential energy curves due to Walji et al. (2015).

2 METHOD

As with other diatomic systems studied as part of the ExoMol project (Yadin et al. 2012; Barton et al. 2013, 2014; Yorke et al. 2014; Patrascu et al. 2015), we treated NaH using both *ab initio* and experimental data. Walji et al. (2015) used a direct potential fit analysis to generate accurate potential energy curves for the ground and first singlet excited states of NaH ($X^1\Sigma_g^+$ and ‘Avoided Crossing’ $A^1\Sigma_g^+$). These curves (also shown in Fig. 1) were then used as input to the program LEVEL version 8.2 (Le Roy 2007) to produce accurate nuclear motion energy levels, wavefunctions and hence transition intensities. A full discussion of how the potential energy curves were derived can be found in Walji et al. (2015), which also gives a comprehensive survey of previous laboratory work on the spectrum of NaH and NaD. We note that the experimental data used by Walji et al. (2015) to determine their curves is insufficient to characterise the last 1000 cm^{-1} of the excited $A^1\Sigma_g^+$ below dissociation, where the A state undergoes another avoided crossing (Aymar et al. 2009). The dissociation limit of this state was constrained by the atomic limit neglecting spin-orbit coupling (Walji et al. 2015) and ro-vibrational states computed in this region must be considered approximate.

2.1 Dipole Moments

Ab initio dipole moments were computed on a dense, uniformly-spaced grid of 220 points from $r=2.40$ to $r=13.40$ a_0 in steps of 0.05 a_0 . Dipoles were computed as expectation value of a multi-reference configuration interaction (MRCI) calculation using a full valence complete active space model, which distributes the two outer electrons among 5 orbitals, and the aug-cc-pwCV5Z basis set. Orbitals were produced using a state-averaged complete active space self consistent field (CASSCF) which considered both the X and A states. The core 2s2p electrons were correlated at the MRCI stage. A single run takes about 4 minutes.

Figure 2 shows our two diagonal dipole moment curves and the off-diagonal $A-X$ transition moment. The diagonal dipoles have a somewhat unusual shape which is undoubtedly associated with the changing character of the NaH wavefunction as a function of geometry. The dipole moment of ground state NaH has been determined experimentally (Dagdigian 1979), but not particularly accurately. Conversely there have been quite a number of theoretical studies on the problem. The most recent is a comprehensive calculation of all three moments considered here by Aymar et al. (2009), who also provide a comprehensive survey of the previous literature. Our results are in excellent agreement with those of Aymar et al. (2009), who also find the various turning points in the dipole curves which are a feature of our calculations.

Our dipole moment points, which are provided in the supplementary material, were input directly into LEVEL.

3 RESULTS

3.1 Partition Function

Partition functions for NaH and NaD were calculated by summing over all energy levels calculated. Szidarovszky & Császár (2015) have recently shown that inclusion of quasibound (resonance or pre-dissociative) states can influence the partition function sums at higher temperatures. Here we present partition functions for both NaH and NaD obtained by summing both

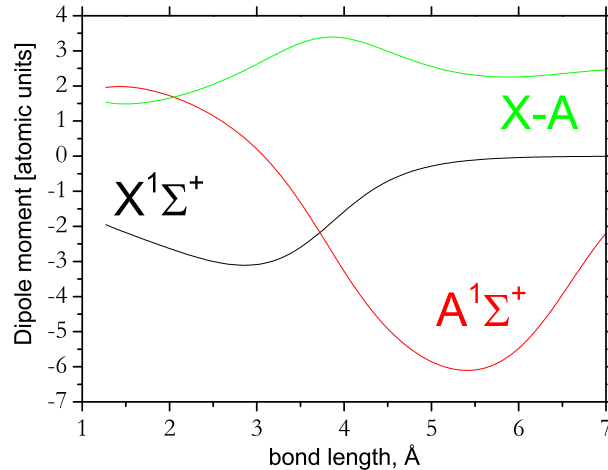


Figure 2. *Ab initio* NaH dipole moment curves as a function of internuclear separation.

over all the truly bound states of the system and also by including quasibound states determined using LEVEL. Table 1 compares these two methods and suggests that below 2000 K the influence of quasibound states on the partition sum can safely be neglected. Above this temperature the quasibound states have a small but increasing influence. However for consistency with our previous work and because we do not consider transitions to quasibound states, we ignore the effect of quasibound states below. For high accuracy work at higher temperatures this approximation may need to be re-visited.

Table 1 also compares our NaH partition functions with those of Sauval & Tatum (1984) and the CDMS database (Müller et al. 2005). Our results cover a larger temperature range: CDMS values only go up to 300 K for NaH, and Sauval & Tatum only claim their values are accurate for 1000 – 9000 K. The latter values were multiplied by the factor 8 in order to explicitly account for the nuclear spin degeneracy in accord with the HITRAN (Fischer et al. 2003) convention, used by ExoMol; the CDMS partition function had to be multiplied by 2. According with the convention of CDMS, the common factors in partition functions are usually divided to keep them small (Müller et al. 2005). After these adjustments results give good agreement with Sauval & Tatum and CDMS in the appropriate temperature ranges, although there is a slight divergence from Sauval & Tatum’s values at higher temperature ranges.

A polynomial fit of this work’s partition functions is given in in Table 2. The values in Table 2 are coefficients in the following equation:

$$\log_{10} Q(T) = \sum_{n=0}^8 a_n (\log_{10} T)^n, \quad (1)$$

which was based on a series expansion used by Vidler & Tennyson (2000).

3.2 Line lists

Line lists were calculated for the two main isotopologues: NaH and NaD. All transitions satisfying the selection rule $\Delta J = \pm 1$ between all ro-vibrational states in the electronic ground state and first electronically-excited state were considered. A summary of each line list is given in Table 3. Although every possible transition was computed, some were very weak and are not included in the final line list.

4 RESULTS

The line lists contain hundreds of thousands of transitions. They are separated into separate energy levels and transitions files. This is done using the standard ExoMol format (Tennyson et al. 2013) where the states file gives all energy levels and associated quantum numbers, and the transitions file gives Einstein A coefficients and the numbers of the associated

Table 1. Partition function of NaH compared with other sources

| $T(K)$ | This work (with quasibound) | This work (without quasibound) | Sauval & Tatum (1984) | CDMS |
|--------|--------------------------------|-----------------------------------|-----------------------|--------|
| 37.5 | | | 51.00 | 45.93 |
| 38 | 46.50 | 46.50 | 51.67 | |
| 75 | 89.10 | 89.10 | 97.98 | 89.10 |
| 150 | 175.73 | 175.73 | 182.99 | 175.72 |
| 225 | 262.83 | 262.83 | 266.93 | 262.62 |
| 300 | 351.39 | 351.39 | 353.94 | 349.79 |
| 500 | 607.74 | 607.74 | 610.87 | |
| 1000 | 1479.85 | 1479.85 | 1460.52 | |
| 1500 | 2764.91 | 2764.89 | 2668.35 | |
| 2000 | 4521.88 | 4520.67 | 4303.28 | |
| 2500 | 6811.55 | 6799.15 | 6437.62 | |
| 3000 | 9692.63 | 9633.66 | 9149.42 | |
| 3500 | 13205.11 | 13024.25 | 12523.04 | |
| 4000 | 17363.28 | 16941.48 | 16649.49 | |
| 4500 | 22161.35 | 21341.29 | 21626.79 | |
| 5000 | 27583.33 | 26178.70 | 27560.23 | |
| 5500 | 33610.90 | 31415.33 | 34562.72 | |
| 6000 | 40227.09 | 37021.39 | 42755.06 | |

Table 2. Fitting parameters for the partition function of NaH/NaD. Fits are valid for temperatures up to 9000 K within 1 %.

| | NaH (with quasibound) | NaH (without quasibound) | NaD (with quasibound) | NaD (without quasibound) |
|-------|--------------------------|-----------------------------|--------------------------|-----------------------------|
| a_0 | 5.20312719799 | -0.19230735479 | -1.61166291473 | -0.19230735479 |
| a_1 | -19.01261024630 | 3.70859873334 | 9.53281763105 | 3.70859873334 |
| a_2 | 34.83255367250 | -3.07887332529 | -13.18395704240 | -3.07887332529 |
| a_3 | -34.37463416770 | 0.71923866264 | 10.40662225870 | 0.71923866264 |
| a_4 | 20.73051960960 | 1.11929540933 | -4.49578453850 | 1.11929540933 |
| a_5 | -7.76051252085 | -0.99902883569 | 1.01674402973 | -0.99902883569 |
| a_6 | 1.75196812228 | 0.34706733327 | -0.09068752170 | 0.34706733327 |
| a_7 | -0.21734537482 | -0.05612884704 | -0.00355980420 | -0.05612884704 |
| a_8 | 0.01134093577 | 0.00348875707 | 0.00081789072 | 0.00348875707 |

Table 3. Summary of the computed NaH and NaD line lists.

| | NaH X state | NaH A state | NaD X state | NaD A state |
|-------------|---------------|---------------|---------------|---------------|
| Maximum v | 21 | 32 | 30 | 34 |
| Maximum J | 81 | 123 | 113 | 171 |

Table 4. Extract from the states file for NaH. The zero of energy is taken to be the energy of the lowest energy level. The files contain 3339 levels for NaH and 5960 levels for NaD.

| n | \bar{E} | g | J | State | v |
|-----|--------------|-----|-----|-------|-----|
| 1 | 0.000000 | 8 | 0.0 | X | 0 |
| 2 | 1133.102453 | 8 | 0.0 | X | 1 |
| 3 | 2228.214399 | 8 | 0.0 | X | 2 |
| 4 | 3285.975269 | 8 | 0.0 | X | 3 |
| 5 | 4306.940010 | 8 | 0.0 | X | 4 |
| 6 | 5291.562054 | 8 | 0.0 | X | 5 |
| 7 | 6240.146564 | 8 | 0.0 | X | 6 |
| 8 | 7152.840057 | 8 | 0.0 | X | 7 |
| 9 | 8029.619734 | 8 | 0.0 | X | 8 |
| 10 | 8870.226718 | 8 | 0.0 | X | 9 |
| 11 | 9674.057941 | 8 | 0.0 | X | 10 |
| 12 | 10440.079797 | 8 | 0.0 | X | 11 |

 n : State counting number. \bar{E} : State energy in cm^{-1} . g : State degeneracy. J : State rotational quantum number. v : State vibrational quantum number.

State: Electronic state label.

Table 5. Extract from the .trans file for NaH. Full tables are available from the Exomol web site www.exomol.com or from the VizieR service from the web site of the Strasbourg Data Center cds.u-strasbg.fr. The files contain 79 898 transitions for NaH and 167 224 transitions for NaD.

| f | i | A_{if} |
|------|------|------------|
| 342 | 322 | 2.1771E+01 |
| 3190 | 3198 | 5.9304E+00 |
| 1168 | 1200 | 6.8873E-01 |
| 3329 | 3327 | 1.1725E+02 |
| 477 | 495 | 5.0419E-01 |
| 3225 | 3217 | 8.4415E+01 |
| 2887 | 2870 | 3.5561E+01 |
| 929 | 938 | 1.0760E-01 |
| 759 | 744 | 1.1033E+01 |
| 3286 | 3280 | 9.6810E+01 |

f : final state number.

i : Initial state number.

A_{if} : Einstein A coefficient in s^{-1} .

Table 6. Lifetimes (in ns) of selected ro-vibrational states within the $A^1\Sigma^+$ electronic state: comparison of experiment Dagdigian (1976); Nedelec (1983) and theory (this work).

| v' | J' | Ref. | Exp. | Calc. |
|------|------|------------------|---------|-------|
| 3 | 8 | Dagdigian (1976) | 24.0(3) | 25.71 |
| 4 | 11 | Dagdigian (1976) | 28.3(3) | 25.69 |
| 5 | 16 | Dagdigian (1976) | 27.1(3) | 26.44 |
| 3 | 4 | Nedelec (1983) | 27 | 25.37 |
| 4 | 6 | Nedelec (1983) | 28.5 | 25.16 |
| 7 | 6 | Nedelec (1983) | 26.5 | 25.40 |
| 9 | 6 | Nedelec (1983) | 26 | 29.71 |
| 11 | 6 | Nedelec (1983) | 25.5 | 33.10 |
| 14 | 7 | Nedelec (1983) | 27 | 36.49 |
| 18 | 11 | Nedelec (1983) | 27.5 | 44.01 |
| 21 | 6 | Nedelec (1983) | 35 | 48.67 |

states. Extracts from the start of the NaH states and transitions files are given in Tables 4 and 5. The full line list can be downloaded from the Exomol web site www.exomol.com or from the VizieR service from the web site of the Strasbourg Data Center cds.u-strasbg.fr. A small computer program which uses these files to compute spectra is given in the supplementary material to Yorke et al. (2014).

The direct potential fit Walji et al. (2015) essentially reproduced all experimental data within its stated uncertainty once a very modest amount of data cleaning had been performed.

Dagdigian (1976), Baltayan et al. (1976) and Nedelec (1983) measured radiative life times for a number of A state ro-vibrational levels. These measurements suggest that the lifetime actually has little dependence on the actual level involved with a sudden increase for $v = 21$. A comparison with our predictions for some of these states is listed in Table 6: in general the agreement is very good. However, in contrast to Nedelec (1983), we observe the increase of the life time of the A state levels at lower vibrational excitations than $v = 21$. The increase is associated with the X state dissociation threshold of 15797.4 cm^{-1} , which truncates the contributions from the bound states of the ground electronic state. Thus the lower experimental values of the life times can be attributed to the transitions to the $X^1\Sigma^+$ quasibound states, which are not included in our line lists.

Figure 3 gives an overview of the entire spectral range covering the X and A systems, from infrared to visible shown as an absorption spectrum generated for $T = 2000 \text{ K}$. Of particular astronomical interest is likely to be the $A - X$ band in the 380 nm region. The $A - X$ band does not exhibit sharp features which can be attributed to the shallow A potential energy curve, see Fig. 1. This reduces the chances of NaH to be detected at visible wavelengths, especially at high temperature, as also illustrated by Fig. 4, where the $A - X$ absorption band is shown for a set of temperatures from 1000 to 4000 K.

Figure 5 shows the pure rotational band of NaH at $T = 298 \text{ K}$ compared to the spectra from the CDMS database. The latter was generated by averaging over the the hyperfine lines, which are not resolved in our line lists. The agreement between intensities can be attributed to the equilibrium X -state dipole moment value of 6.7 D of Sachs et al. (1975) used by CDMS. Our value is 6.43 D at $r_e = 1.887$.

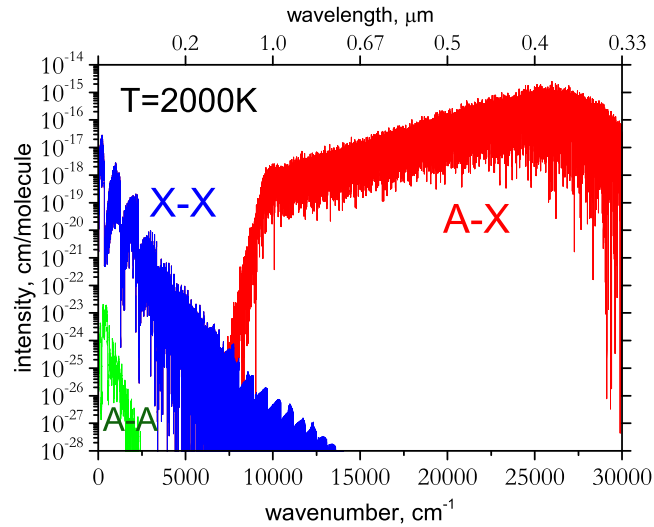


Figure 3. Overview of the X–X, A–A, and A–X absorption spectrum of ^{23}NaH at 2000 K. The theoretical spectrum is convolved with a Gaussian profile with a half-width half-maximum (HWHM) of 0.1 cm^{-1} .

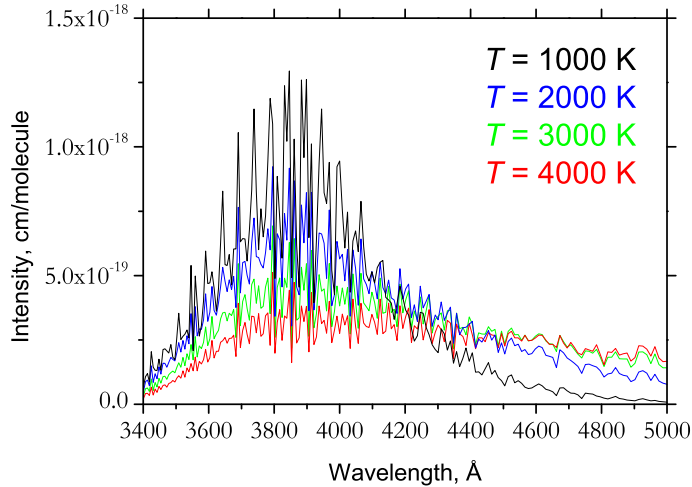


Figure 4. Computed A–X absorption spectrum of ^{23}NaH at different temperatures. A Doppler profile was used to convolve the theoretical spectrum. Wavenumber bin of 50 cm^{-1} was chosen to mimic resolving power of about 500 to 1000.

5 CONCLUSIONS

We present comprehensive line lists for NaH and NaD. These are based on the direct solution of the nuclear motion Schrödinger equation using potential energy curves obtained by fitting to experimental data of measured transitions, all calculated by Walji et al. (2015). These were combined with a new *ab initio* dipole moment curve to produce comprehensive line lists for these two species. The strong A–X feature about 380 nm should provide a signature for NaH in the atmospheres of cool stars, brown dwarfs and exoplanets. However, the shallow nature of the upper $A^1\Sigma^+$ electronic state means that this feature is predicted to be rather broad. While this means that NaH can make a significant contribution to the opacity, it is likely to make this feature difficult to detect.

NaH was recently identified one of only two key diatomic species whose spectral data was completely missing from M-dwarf models (Rajpurohit et al. 2013). A study on the other of these species, AlH, has just been completed and will be reported soon.

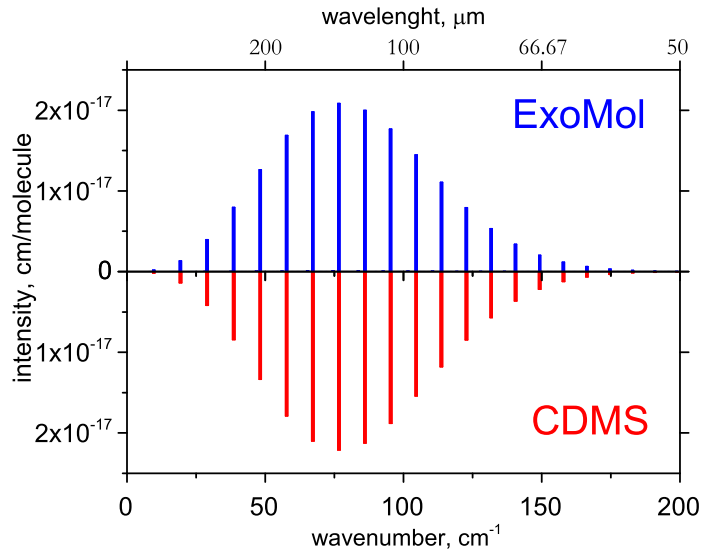


Figure 5. Rotational spectrum of ^{23}NaH computed at $T = 298\text{ K}$: ExoMol (current work) and CDMS (Müller et al. 2005). The CDMS intensities were obtained by summing individual hyperfine transitions; these were generated by Müller et al. (2005) using an equilibrium dipole moment of 6.7 D as calculated by Sachs et al. (1975).

ACKNOWLEDGEMENTS

This work was supported by the ERC under the Advanced Investigator Project 267219 and a Wolfson Royal Society Research Merit award.

REFERENCES

- Aymar M., Deiglmayr J., Dulieu O., 2009, *Can. J. Phys.*, 87, 543
 Baltayan P., Jourdan A., Nedelec O., 1976, *Phys. Lett. A*, 58, 443
 Barton E. J., Chiu C., Golpayegani S., Yurchenko S. N., Tennyson J., Frohman D. J., Bernath P. F., 2014, *MNRAS*, 442, 1821
 Barton E. J., Yurchenko S. N., Tennyson J., 2013, *MNRAS*, 434, 1469
 Czarny J., Felenbok P., Roueff E., 1987, *A&A*, 188, 155
 Dagdigian P. J., 1976, *J. Chem. Phys.*, 64, 2609
 Dagdigian P. J., 1979, *J. Chem. Phys.*, 71, 2328
 Fischer J., Gamache R. R., Goldman A., Rothman L. S., Perrin A., 2003, *J. Quant. Spectrosc. Radiat. Transf.*, 82, 401
 Juarros E., Pellegrini P., Kirby K., Cote R., 2006, *Phys. Rev. A*, 73, 041403
 Kirby K., Dalgarno A., 1978, *ApJ*, 224, 444
 Le Roy R. J., 2007, LEVEL 8.0 A Computer Program for Solving the Radial Schrödinger Equation for Bound and Quasibound Levels. University of Waterloo Chemical Physics Research Report CP-663, <http://leroy.uwaterloo.ca/programs/>
 Leopold K. R., Zink L. R., Evenson K. M., Jennings D. A., 1987, *J. Mol. Spectrosc.*, 122, 150
 Müller H. S. P., Schlöder F., Stutzki J., Winnewisser G., 2005, *J. Molec. Struct. (THEOCHEM)*, 742, 215
 Nedelec, O. and Giroud M., 1983, *J. Chem. Phys.*, 79, 2121
 Okabayashi T., Tanimoto M., 2000, *ApJ*, 543, 275
 Patrascu A. T., Tennyson J., Yurchenko S. N., 2015, *MNRAS*
 Plambeck R. L., Erickson N. R., 1982, *ApJ*, 262, 606
 Rajpurohit A. S., Reyle C., Allard F., Homeier D., Schultheis M., Bessell M. S., Robin A. C., 2013, *A&A*, 556, A15
 Sachs E. S., Hinze J., Sabelli N. H., 1975, *J. Chem. Phys.*, 62, 3367
 Sauval A. J., Tatum J. B., 1984, *ApJS*, 56, 193
 Snow T. P., Smith W. H., 1977, *ApJ*, 217, 68
 Su Q., Yu J., Niu Y., Cong S., 2010, *Chem. Phys. Lett.*, 27, 3401
 Szidarovszky T., Császár A. G., 2015, *J. Chem. Phys.*, 142, 014103

- Tennyson J., Hill C., Yurchenko S. N., 2013, in AIP Conference Proceedings, Vol. 1545, 6th international conference on atomic and molecular data and their applications ICAMDATA-2012, AIP, New York, pp. 186–195
- Tennyson J., Yurchenko S. N., 2012, MNRAS, 425, 21
- Vidler M., Tennyson J., 2000, J. Chem. Phys., 113, 9766
- Walji S.-D., Sentjens K., Roy R. J. L., 2015, J. Chem. Phys., submitted
- Weisstein E. W., Serabyn E., 1996, Icarus, 123, 23
- Yadin B., Vaness T., Conti P., Hill C., Yurchenko S. N., Tennyson J., 2012, MNRAS, 425, 34
- Yang C. L., Zhang X., Han K. L., 2004, J. Molec. Struct. (THEOCHEM), 676, 209
- Yorke L., Yurchenko S. N., Lodi L., Tennyson J., 2014, MNRAS, 445, 1383